

RESEARCH ARTICLE

10.1029/2018JD029094

Special Section:

Water-soil-air-plant-human nexus: Modeling and observing complex land-surface systems at river basin scale

Key Points:

- Comparison of long-range correlations of soil moisture between the shady slope and sunny slope. Comparison of long-range correlations of soil temperature between the shady slope and sunny slope. Comparison of long-range cross correlation between the soil moisture and soil temperature between the shady slope and sunny slope
- Long-range correlation and long-range cross correlation display vertical depth variation and timescale variation
- We seek out driving factors of stratification heterogeneity of LRC and LRCC in different soil depths

Correspondence to:

C. Cheng, C. Song, and S. Ye, chencx@bnu.edu.cn; songcq@bnu.edu.cn; yesj@bnu.edu.cn

Citation:

Zhang, T., Shen, S., Cheng, C., Song, C., & Ye, S. (2018). Long-range correlation analysis of soil temperature and moisture on A'rou hillsides, Babao River Basin. *Journal of Geophysical Research: Atmospheres*, 123. <https://doi.org/10.1029/2018JD029094>

Received 31 MAY 2018

Accepted 1 OCT 2018

Accepted article online 24 OCT 2018

Long-Range Correlation Analysis of Soil Temperature and Moisture on A'rou Hillsides, Babao River Basin

Ting Zhang^{1,2,3} , Shi Shen^{1,2,3} , Changxiu Cheng^{1,2,3} , Changqing Song^{1,3}, and Sijing Ye^{1,2,3}

¹State Key Laboratory of Earth Surface Processes and Resource Ecology, Beijing Normal University, Beijing, China, ²Key Laboratory of Environmental Change and Natural Disaster, Beijing Normal University, Beijing, China, ³Center for Geodata and Analysis, Beijing Normal University, Beijing, China

Abstract Studying the tendency of soil temperature and moisture can provide scientific support for setting soil parameters for land surface hydrological model. Previous research has shown that there is long-range correlation of soil temperature or moisture; however, driving factors of long-range correlation variations and the cross correlation between temperature and moisture under multiple timescales have rarely been discussed. To explore the driving factors, we compared long-range correlation between shady and sunny slopes. Adaptive fractal analysis was utilized to analyze long-range cross correlation (LRCC) and long-range correlation (LRC). Experimental data were collected between 9 August 2013 and 3 December 2014 at A'rou observation stations, Babao River Basin. Results show that two slopes have some common characteristics. (1) Soil temperature and moisture display the consistent change. (2) The persistence intensity of moisture, temperature, and their interaction intensity change at 9, 6, and 6-day timescales, respectively. (3) LRC and LRCC indices demonstrate the stratification heterogeneity. Results also show that LRC and LRCC indices on two slopes have differences. The soil system was stratified into three layers to explain these differences over large timescales. (1) At 4- to 20-cm depth, with significant influence of solar radiation and evapotranspiration on sunny slope, moisture shows weaker persistence. There is stronger antipersistence of temperature and stronger hydrothermal interaction on sunny slope. (2) At 20- to 80-cm depth, there is weaker persistence of soil moisture on shady slope because of unstable groundwater and side runoff supply. (3) At 80- to 160-cm depth, with seasonal melt-water effect on sunny slope, persistence of moisture was considerably weaker.

1. Introduction

The exchange and balance of water, heat, and gas are frequent between the soil system and the atmosphere near the Earth's surface (Katul et al., 2012). Soil temperature and soil moisture are two important variables in the soil-atmosphere circle (Wu et al., 2010). Soil moisture can affect the energy exchange process between land and air through latent heat and sensible heat conduction, and then influence the local climate (Chahine, 1992). Additional, soil moisture and soil temperature are closely related to some meteorological factors, including solar radiation (SR; Xiaoning Song et al., 2013), evaporation (Sorman & Abdulrazzak, 2010), and precipitation (Koster et al., 2004). Research on soil moisture and soil temperature mostly concentrate on their spatial distribution patterns (Kim & Singh, 2014; Yang et al., 2015), evolution trend with time (Albergel et al., 2013; Sheffield & Wood, 2010), and their relationship with other environmental and factors (Che et al., 2018; Ding et al., 2017; Green et al., 2010).

However, the stratification heterogeneity of soil temperature and soil moisture evolution trend is rarely discussed. And the driving factors of this stratification heterogeneity are insufficiently discussed. The LRC analysis was mostly used to depict the evolution trend of soil moisture time series (Biswas et al., 2012; Shen et al., 2018; Wang et al., 2010). Gao et al. (2015) claimed that the persistence of soil moisture increased with depth in the agro-ecosystem of Luancheng, whereas Song et al. (2011) noted that the persistence of soil moisture was not consistent with depth change. Obviously, the persistence of soil moisture displays soil depth variation, while driving factors are insufficiently discussed. Tang et al. (2012) suggested that soil temperature had a significant positive correlation with depth in the middle of the Qilian Mountains. The research of Che et al. (2018) showed that the response of soil temperature to meteorological elements was different at different soil depths. It is apparent that soil temperature series characteristics displays soil depth variation, but the driving factors are still unclear. To discuss the driving factors of this stratification

heterogeneity, the persistence of soil moisture and soil temperature in different SR conditions were compared in this paper.

Another goal of this research is to reveal the cross correlation between temperature and moisture under multiple timescales and multiple depths. Soil temperature and soil moisture are not independent (Han et al., 2016). Analysis of intrinsic correlation between soil temperature and soil moisture can help to understand hydrothermal interactions (Seneviratne et al., 2010). The research of Che et al. (2018) showed that the soil temperature was significantly relative to soil moisture in the Shanxi section of the Qilian. Stearns and Carlson (1960) and Lakshmi et al. (2010) also analyzed the linear relationship between soil temperature and soil moisture. However, the traditional linear correlation analysis ignores the timescale dependence of correlation. In our research, the LRCC analysis was applied to explore the evolutionary trend between two sequences under multiple timescales at different depths. And we also compared the results of LRCC analysis under different SR conditions. Through studying hydrothermal interaction process, the evolutionary trend characteristics of soil moisture and temperature series under partial depth and timescales can be illustrated.

As a part of climate-hydrological system, soil temperature and soil moisture have many complex properties such as hierarchy, self-similarity, and dynamics (Joelson et al., 2016; Mandelbrot & Wallis, 1995). In addition, time series of them exhibit incomplete random fluctuation with periodic change and present nonlinear properties (Goodchild & Mark, 2015; SONG Changqing et al., 2018; CHENG Changxiu et al., 2018). The LRC analysis can be used to quantitatively describe the statistical serial correlation (persistence) of this type of nonlinear sequence (Mandelbrot, 1991). The LRCC analysis can quantitatively explore the interaction between two sequences of specific timescale (Podobnik et al., 2011).

It is very important to quantitatively characterize the evolution trend of soil moisture and soil temperature and evaluate the predictability of them. It can provide the basis for setting the soil parameters in terrestrial climate, ecological, and hydrological models (Porporato et al., 2002; Williams, 2013). In this paper, we calculated the LRC indices (H) of soil moisture and LRC indices (H) of temperature at different depths. Furthermore, H can reflect the intensity of persistence or antipersistence of soil moisture time series at a certain timescale. For persistent series, the noise level is low and the trend is obvious; for antipersistent series, the noise level is high and the trend is weak. LRCC indices (H_{cor}) between soil moisture and soil temperature were also calculated at different depths. Furthermore, H_{cor} can reflect the intensity of consistent or inconsistent change between the two series at a certain timescale. That is, H_{cor} depicts the intensity of hydrothermal interaction at certain depth and timescale. These indices reflect the evolution trend of soil temperature and soil moisture.

In addition, in the framework of the climate change, the drought trend will include arid areas becoming more arid and wetter areas becoming wetter (Dai, 2013; Trenberth et al., 2014). Through characterizing the evolution trend of soil temperature and soil moisture under multiple timescales, LRC and LRCC results of soil moisture and soil temperature can contribute to understand the current drought process and predict the drought trend in the future (Sheffield & wood, 2010; Song et al., 2017).

In the following section (section 2), we will describe the study area and introduce the experimental data. Research methods will be introduced in section 3. Results of the research are presented and analyzed in section 4. Section 5 comprises discussions and major conclusions.

2. Study Area and Data

2.1. Study Area

The research area is on shady slope and sunny slope at the A'rou observation station, which is located upstream of a hydro-meteorological observation network in the Heihe River Basin. The observation field is stationed in the highlands of the river valley on the south side of the Babao River. The Babao River is tributary in the upper reaches of the Heihe River, which belongs to Qilian County of Qinghai Province in the town of A'rou.

There are more precipitation and glacier melt water supply in the upper reaches of Qilian mountainous area, which is the runoff formation area of Heihe. Qilian mountainous area is the mainly runoff formation area of the Heihe River. The total basin area of the Babao River is 2,452 km². The average annual temperature is 0.7 °C, average annual precipitation is approximately 400 mm, and average amount of evaporation is 1,529.8 mm (Li et al., 2014). During the winter, the climate in the basin is cold and dry and snowfall occurs

less, and there is sufficient sunshine and strong SR. During the summer, the climate in the basin is cool and humid. Runoff is mainly supplied by precipitation and is supplemented by meltwater and streams. Water resources in this basin are mainly restricted by precipitation and temperature.

The details of the two stations are the following. The sunny slope station is located at 100.5204°E, 38.0898°N, north of A'rou, and 3,529 m above sea level. The slope angle of sunny slope is 6.13°. The slope direction is 258.69 (clockwise direction relative to the north). The shady slope station is located at 100.4108°E, 37.9841°N, south of A'rou, and 3,536 m above sea level. The slope angle of shady slope is 13.14°. The slope direction is 28.30 (clockwise direction relative to the north). The slope angle mainly affects the infiltration rate of rainfall. The total precipitation during the whole research period in both the two stations was less than 5 mm. And there is little difference in the precipitation distribution between the two stations in the whole research period. Therefore, in this research, the difference of slope between the two stations will not be the significant driver to different persistence of soil temperature and moisture. The underlying surface of these two observation sites is alpine meadow, and the soil type of these two observation sites is Matti-Gelic Cambosols (China Soil Taxonomy, CST). Therefore, soil type and vegetation type will not be the major driver to different persistence of soil temperature and moisture. It is apparent that sunny slope station is closer to the runoff (Figure 1). Less runoff is distributed around the shady slope station. Therefore, water supply for sunny slope is more stable than that for shady slope. In addition to the SR condition and runoff distribution, there is no significant difference between the two slopes in terms of geographical location, altitude, climate, surface coverage, and other natural conditions.

2.2. Data

The research data set contains soil moisture and temperature observation data from 9 August 2013 to 3 December 2014. The data set was obtained from the Heihe eco-hydrological remote sensing test (HiWATER). The soil moisture in this paper is the soil volumetric water content (%), and the measurement of temperature is in Celsius (°C). The probes for soil temperature and moisture are buried underground at depths of 4, 10, 20, 40, 80, 120, and 160 cm, which is located 2 m south of the weather tower. The detailed information for this data set can be seen in the research of Li et al. (2013) and Liu et al. (2011). The following study divides the soil into three layers: the shallow layer corresponding to 4- to 20-cm depths, the middle layer corresponding to 20- to 80-cm depths, and the deep layer corresponding to 80- to 160-cm depths.

3. Methods

3.1. Data Preprocessing

The observation interval of soil temperature and moisture in the original data set is 10 min. After removing the invalid data, the daily average series of the original series is calculated for the following LRC and LRCC analysis. The daily average series of soil moisture and temperature can be written as $\{m_j^i\}$ and $\{t_j^i\}$ respectively, where j denotes soil depth and i denotes time.

3.2. Long-Range Correlation Analysis

The Hurst exponent (H) was first proposed in the study of a ribonucleic acid sequence by Peng et al. (1994). In the LRC analysis of nonlinear processes, H is an important index used to quantify the long memory and depict the statistical correlation of the time series. In the present study, detrended fluctuation analysis (DFA) and AFA are mostly used to fit H .

While, AFA is better than DFA on dealing with arbitrary and strong nonlinear trends (Gao et al., 2011). By constructing overlapped sliding fitting windows, the AFA algorithm has the following advantages. (1) It can extract the global smoothing trend more accurately and effectively remove the self-circulation and external trend of the series (Riley et al., 2012). (2) It obtains better scaling in the variance of the magnitude of residuals $F(w)$ versus the length of the window w dependence (Gao et al., 2012). (3) It can give more reliable long-range correlation results (Gao et al., 2011). However, due to the noncoincidence of each fitting window, there is abrupt change at the boundary of adjacent segments and unsmooth trend for the general series in the DFA algorithm. Meanwhile, in the research of Gao et al. (2012) about long-range correlations of social and natural phenomena, H was fitted by AFA and DFA, respectively. Finally, they rely on the results of AFA for final interpretation. In addition, AFA algorithm has also been used in many fields, such as fractal analysis of bio-

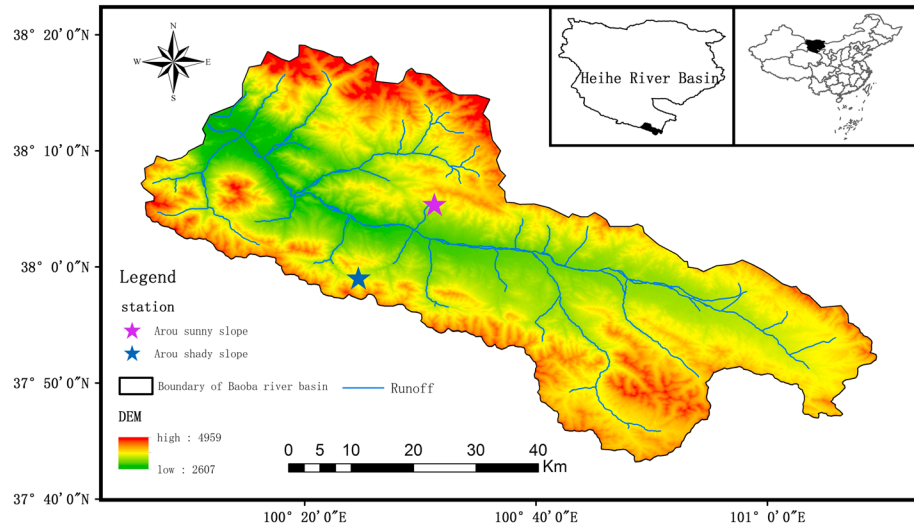


Figure 1. Geographical location of the research area.

signals (Gao, Lasch, & Chen, 2013), political conflict (Gao, Leetaru, et al., 2013; Gao et al., 2017), and traffic volume (He et al., 2016).

Therefore, AFA algorithm was used to estimate the H of soil temperature and moisture series in this study. These series belong to the random walk process. The specific process of fitting H is as follows:

- (1) The sliding window (w) is structured to fit the trends of $\{t_i\}$ and $\{m_i\}$. In the fitting process, the size of each segment window can be written as $w = 2n + 1$; there are $n + 1$ points overlapped between two adjacent windows. Each window is fitted by M order polynomials, $M = 1$ in this study. The fitting results of segments i and $i + 1$ are recorded as $y^{(i)}(l_1)$ and $y^{(i+1)}(l_2)$, respectively. Then, the fitting results for the overlapped region are defined as $y^{(c)}(l)$. Weighted fitting is based on the distance between the overlapped parts and original series.

$$y^{(c)}(l) = w_1 y^{(i)}(l + n) + w_2 y^{(i+1)}(l), l = 1, 2, \dots, n + 1 \quad (1)$$

where $w_1 = 1 - d_1/n$; $w_2 = 1 - d_2/n$; d_1 and d_2 represent the distance between the fitting points and the actual point in the overlapping part, respectively.

After each segment and each overlapped region have been fitted, the global trends of soil temperature and moisture can be denoted as $\{at_i\}$ and $\{am_i\}$, respectively.

- (2) The detrended series (the residual of the original series to the global trend) for soil temperature and moisture can be structured as $t(i) - at(i)$ and $m(i) - am(i)$, respectively. The root mean square residual at a certain window size (w) can be denoted as $F(w)$. The relation between the $F(w)$ and w yields the H according to

$$F_1(w) = \sqrt{\frac{1}{N} \sum_i^N (t(i) - at(i))^2} \sim w^{H_1} \quad (2)$$

$$F_2(w) = \sqrt{\frac{1}{N} \sum_i^N (m(i) - am(i))^2} \sim w^{H_2}$$

where H_1 and H_2 represent the Hurst exponents of soil temperature and moisture, respectively.

- (3) Under double logarithmic coordinates of $F(w)$ and w , H_1 and H_2 are the slope of a linear fitted by the ordinary least squares. Timescale ranges of H can be identified by the coverage range of w corresponding to the slope.

H can be used to describe persistence or antipersistence of a series. $H = 0.5$ indicates that the sequence is a random process (white noise). This indicates that the points have no correlation with each other (with short

memory only); $0.5 < H < 1$ indicates the series shows persistence. With the increase of H , the increments in the series are more likely to be followed by further increases. The intensity of persistence peaks at $H = 1$; $0 < H < 0.5$ indicates that the series shows antipersistence. With the decrease of H , the increments in the series are more likely to be followed by decreases. The intensity of antipersistence peaks at $H = 0$. Furthermore, for persistent series, the noise level is low and the trend is obvious; for antipersistent series, the noise level is high and the trend is weak.

3.3. Long-Range Cross Correlation Analysis Based on AFA

The LRCC algorithm was first proposed by Podobnik and Stanley (2008). This algorithm uses covariance for two series in the LRC analysis to carry out multiple timescale cross correlation analysis. In this study, the cross-correlation exponent (H_{cor}) is calculated based on the trend extracted by the above AFA algorithm. The specific algorithm is as follows:

- (1) The detrended soil temperature and moisture series are obtained by calculating the difference between the original series and global trend, respectively. $F_{\text{cor}}(w, m, t)$ is obtained through the covariance of two detrended series:

$$F_{\text{cor}}(w, m, t) = \sqrt{\frac{1}{N} \sum_i^N (m(i) - am(i))(t(i) - at(i))} \sim w^{H_{\text{cor}}} \quad (3)$$

- (2) Under double logarithmic coordinates of F_{cor} and w , H_{cor} is the slope of a linear fitted by ordinary least squares. Timescale ranges of H_{cor} can be identified by the coverage range of w corresponding to the slope.

H_{cor} can be used to describe the consistent or inconsistent change between two series. $H_{\text{cor}} = 0.5$ indicates that two series are independent from each other and have no cross correlation; $0.5 < H_{\text{cor}} < 1$ indicates that one series presents a consistent change with the other. With the increase of one series, the increments are more likely to be found in the other series. The intensity of consistency peaks at $H_{\text{cor}}=1$; $0 < H_{\text{cor}} < 0.5$ is the opposite, and the intensity of inconsistency peaks at $H_{\text{cor}} = 0$.

4. Results and Analysis

The fluctuation of soil moisture or temperature time series is not completely random. And, LRC of soil moisture or temperature presents a vertical depth variation and timescale variation. The variation mainly includes two aspects: persistence and intensity.

The soil temperature series and the soil moisture series at the same depth are not independent. LRCC between these two series also presents the vertical depth variation and timescale variation. The variations of LRCC also contain consistency and intensity.

To discuss the possible driving factors of these variations, the next section will compare the LRC results and LRCC results between the sunny slope and shady slope.

4.1. The Diffidence in the LRC Results of Soil Moisture Between the Two Slopes

This section applied the AFA (section 3.2) to fit H of soil moisture. The LRC indices of the two slopes are plotted in Figure 2. The fluctuation of these series is persistent at most depth. However, at a specific depth and specific timescale, LRC indices of the two slopes are different. There is an obvious linear relationship between $F(w)$ and w under the double logarithmic coordinates in each plot, and the slopes (H) are between 0.5 and 1 at most depth. In addition, there is an inflection point in fitting H at each depth and H is varied with depth. This research focuses on the slow scaling region of soil moisture and soil temperature. The point with lower root-mean-square error (no more than 0.02 of the minimum of root-mean-square error) and smaller corresponding timescale is selected as the inflection point at each depth, so that the timescale of the second interval is more extensive. This means that the LRC of soil moisture displays timescale variation and vertical depth variation.

From Figure 2, for the two slopes, the intensity of the soil moisture persistence both mutates at 9 days on the timescale. There is the same timescale variation of soil moisture LRC at the two slopes. $F(w)$ of soil moisture

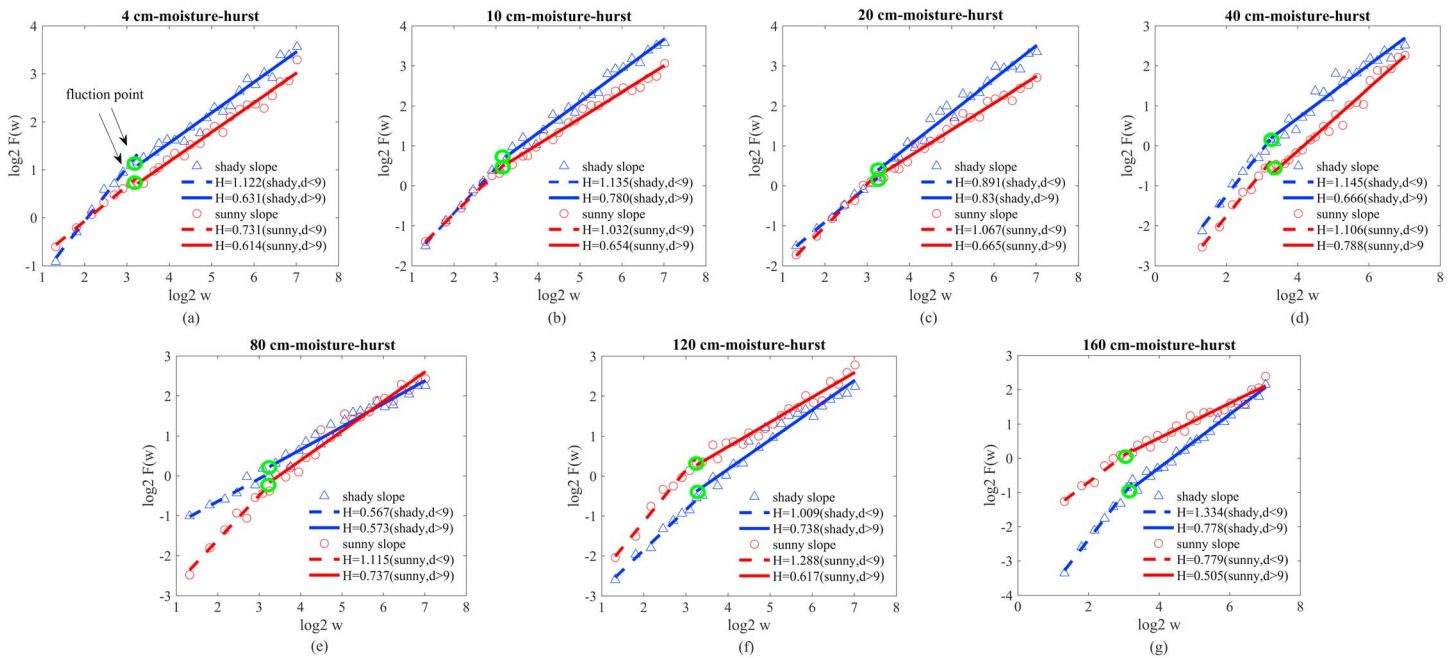


Figure 2. Adaptive fractal analysis results plot for soil moisture series in each layer for the sunny slope and shady slope. The above plots (a–g) are from AFA using a polynomial order of $M = 1$. The AFA plot is a plot of $\log_2 F(w)$, as a function of $\log_2 w$ (w corresponding to the timescale). The point of the soil moisture in shady slope is represented by the blue triangle, and the point of soil moisture in sunny slope is represented by the red circle. The value of H is the slope of the line. There are two slopes for each depth, and the inflection point is the last point of the first interval (i.e., the green circle in figure (a)). Inflection point exists at $\log_2 w = 3.2479$ at each depth. H fitted by dashed line covers a small timescale ($2 < d < 9$), and H fitted by solid line covers a large timescale ($d > 9$).

can be fitted two H indices (slopes). Both on the two slopes, the slow scaling region covers the time windows $\log_2 w$ over 3.248, which corresponds to the actual time range over 9 days. H indices are between 0.5 and 1. Therefore, soil moisture series at this scaling region presents persistence. Both on the two slopes, the fast scaling region covers time windows from 1.322 to 3.248 (2- to 9-day estimates). H indices are higher than 1 at most depths in this scaling region. It is indicated that the relationship between the future trend and the past trend of soil moisture cannot be explained by the LRC analysis, in addition to 4, 160-cm depths at the sunny slope and 20, 80-cm depth at the shady slope.

The persistence of soil moisture is mainly displayed in a slow scaling region. To analyze the vertical depth variation of the soil moisture LRC at the two slopes, H of the slow scaling region at the two slopes was plotted in Figure 3a. The average soil moisture of the entire study period was calculated as a reference, and the results of the two slopes are described in Figure 3b.

From Figure 3a, both on the sunny slope and shady slope, H indices of soil moisture are various among different depths in the slow scaling region. However, there is different vertical depth variation feature at the two slopes. For the sunny slope, H increases with depth from 4 to 40 cm and peaks at 40-cm depth ($H = 0.788$); H decreases with depth from 40- to 160 cm. The soil moisture series of 160-cm depth is similar to white noise ($H = 0.505$). For the shady slope, H increases with depth in both shallow and deep layers. The 20-cm depth shows the most significant persistence ($H = 0.891$); H decreases with depth in middle layer and has the weakest persistence ($H = 0.573$) at 80-cm depth. It is illustrated that the intensity of persistence does not simply ascend or descend with depth. In general, the above results indicate that the persistence of soil moisture for the shady slope is stronger than that of the sunny slope. In addition, this phenomenon is more obvious in the shallow layer.

4.2. The Diffidence in the LRC Results of Soil Temperature Between the Two Slopes

This section applied the AFA (section 3.2) to fit H of soil temperature. The LRC indices of the two slopes are plotted in Figure 4. At a specific depth and specific timescale, LRC indices of the two slopes are different.

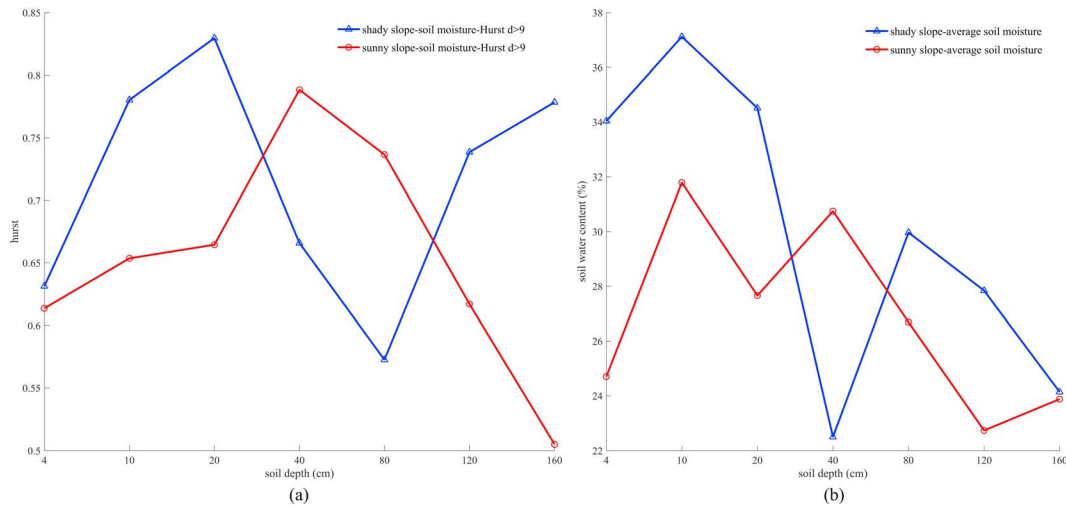


Figure 3. (a and b) Comparison of soil moisture H and average soil moisture between the sunny slope and shady slope. In figure a, the longitudinal axis represents the H value of soil moisture in the slow scaling region (over 9 days), and the horizontal axis represents different soil depths. The red and blue lines correspond to the results of different sunshine conditions, sunny slope, and shady slope, respectively. In figure b, the longitudinal axis represents the average soil moisture (unit is volumetric water content %) for the entire study period (9 August 2013–3 December 2014), and the horizontal axis represents different soil depths. The red and blue lines correspond to the results of different sunshine conditions, sunny slope, and shady slope, respectively.

There is an obvious linear relationship between $F(w)$ and w under the double logarithmic coordinates in each plot. In addition, there is an inflection point in fitting H at each depth and H is also varied with depth. This indicates that the LRC of soil temperature displays timescale variation and soil depth variation.

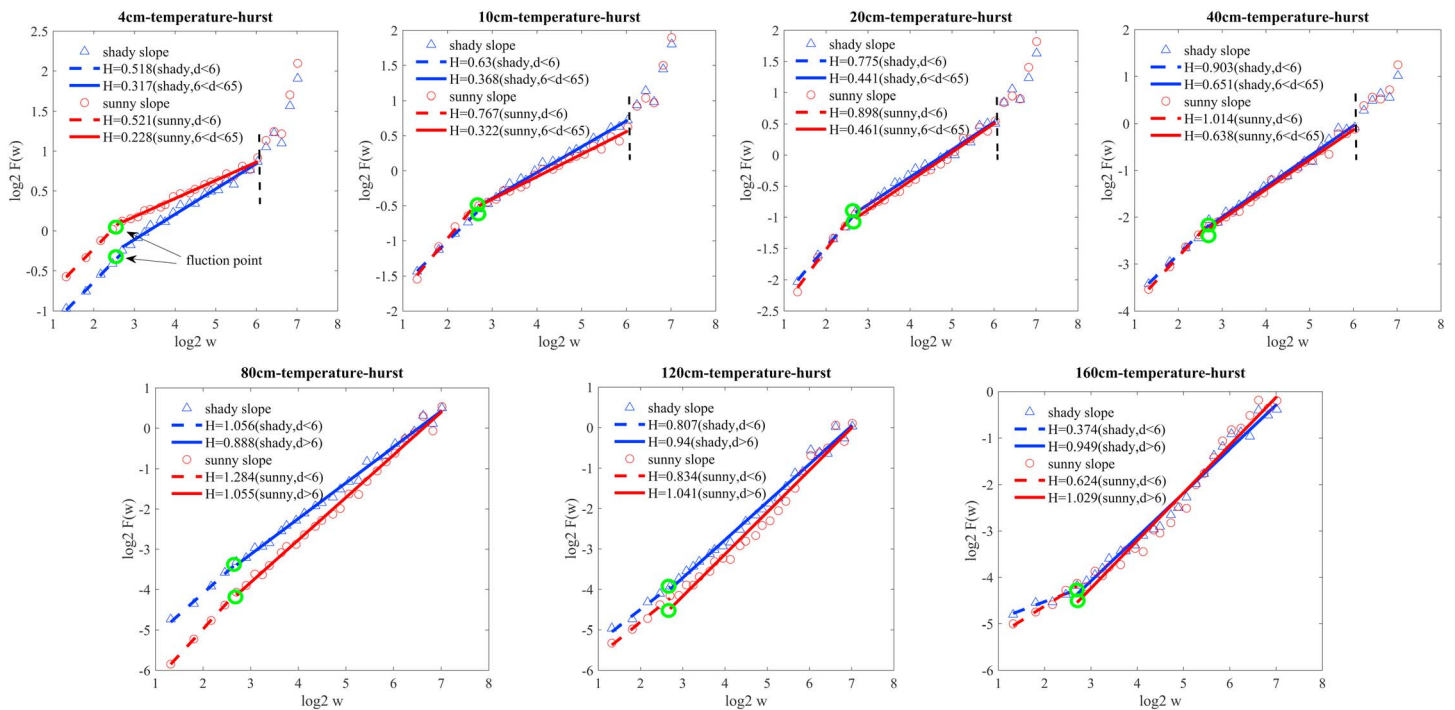


Figure 4. (a–g) Adaptive fractal analysis plots for soil temperature series in each layer for the sunny slope and shady slope. The above plots (a–g) are from adaptive fractal analysis using a polynomial order of $M = 1$. The point of the soil temperature in shady slope is represented by the blue triangle, and the point of soil temperature in sunny slope is represented by the red circle. The value of H is the slope of the line. There are two slopes for each depth, and the inflection point is the last point of the first interval (i.e., the green circle in figure (a)). Inflection point exists at $\log_2 w = 2.7004$ at each depth. H fitted by dashed line covers a small timescale ($2 < d < 6$). For depths 4–40 cm, H fitted by solid line covers a timescale range of $6 < d < 65$. And the points after the black vertical dotted line belong to the third region. For depths 80–160 cm, H fitted by solid line covers a timescale range over 65 days.

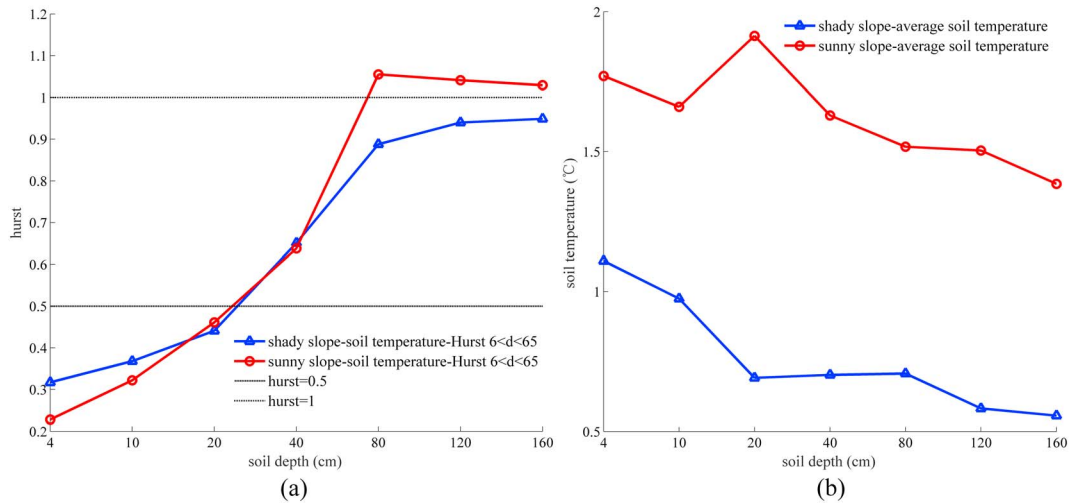


Figure 5. (a and b) Comparison of soil temperature H and average soil temperature between the sunny slope and shady slope. In figure a, the longitudinal axis represents the value of the H of soil temperature in the slow scaling region (6–65 days), and the horizontal axis represents different depths. The red and blue lines correspond to the results of different sunshine conditions, sunny slope, and shady slope, respectively. In figure b, the longitudinal axis represents the average soil temperature of the entire study period (9 August 2013 to 3 December 2014), and the horizontal axis represents different depths. The red and blue lines correspond to the results of different sunshine conditions, sunny slope, and shady slope, respectively.

From Figure 4, for the sunny slope and shady slope, the persistence and intensity of the soil temperature fluctuation both mutate at 6 days on the timescale. There is the same timescale variation of soil temperature LRC at the two slopes. H indices of soil temperature at 4- to 40-cm depths contain three scaling regions. The fast scaling region covers time windows $\log_2 w$ from 1.3219 to 2.7004, which corresponds to an actual range of 2–6 days. The slow scaling region covers time windows of 2.7004–6.0334 (6- to 65-day estimates). Because the timescales in the third region is too small for linear fitting, the third region (time windows over 6.0334) is not discussed in this research. H indices of soil temperature at 80- to 160-cm depths contain two scaling regions. The fast scaling region covers 2–6 days. The slow scaling region covers the range over 6 days. H indices of soil temperature in the fast scaling region are higher than 0.5. It is indicated that there is persistence of soil temperature in small timescale. Both on shady and sunny slope, the timescale variation of the soil temperature LRC is most remarkable at shallow layer. There is antipersistence in the large timescale and persistence at the small timescale at this layer.

The LRC of soil temperature in the slow scaling region (6–65 days) will be mainly discussed in this section. To analyze the vertical depth variation of soil temperature LRC, H of the slow scaling region at two slopes was plotted in Figure 5a. The average soil temperature of the entire study period was calculated as a reference in Figure 5b.

From Figure 5a, on both shady and sunny slopes, H indices of soil temperature are various among different depths in the slow scaling region. Meanwhile, H of the soil temperature basically increases with depth at the two slopes. The intensity of antipersistence for the sunny slope is stronger than that of the shady slope. For the sunny slope, soil temperature displays the antipersistence in shallow layer. The antipersistence weakens with the depth. The strongest antipersistence is shown at 4-cm depth with $H = 0.228$. The weakest antipersistence ($H = 0.461$) can be found at 20-cm depth. Soil temperature displays the persistence at 40-cm depth. For the shady slope, the vertical stratification structure of H is similar to that in the sunny slope. There is the strongest antipersistence ($H = 0.317$) at 4-cm depth. The weakest antipersistence ($H = 0.441$) is at 20-cm depth. The persistence peaks at 80- and 120-cm depths with approximately $H = 1$. The above results reveal that the persistence intensity of soil temperature increases with depth and the antipersistence intensity decreases with depth, especially on the shady slope. In addition, there is stronger antipersistence of soil temperature in the sunny slope. This phenomenon is more obvious at 4 cm.

4.3. The Diffidence in the LRCC Results Between the Two Slopes

This section applied the LRCC analysis method (section 3.3) to fit the H_{cor} between the soil temperature and moisture. LRCC indices of the two slopes were plotted in Figure 6. There is consistency between the soil

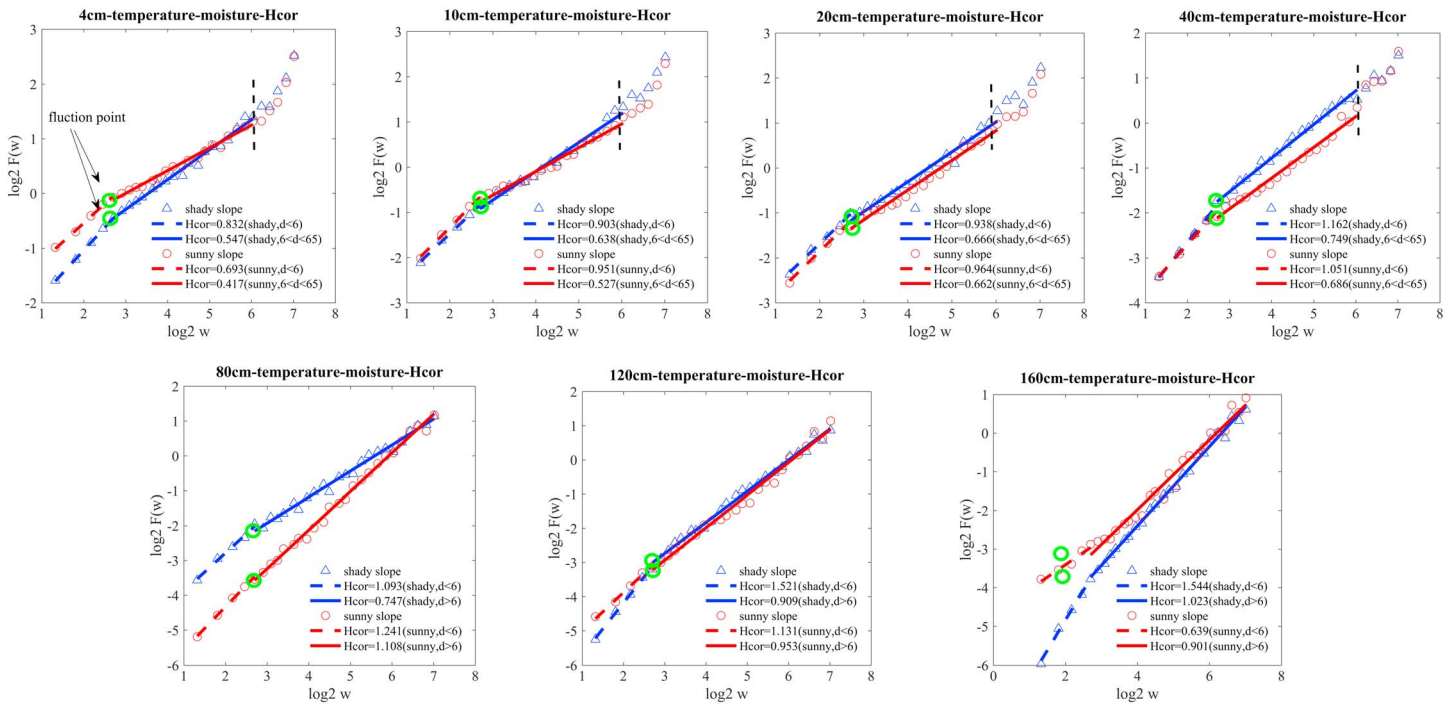


Figure 6. (a–g) Long-range cross correlation results plot between the soil moisture series and soil temperature series in each layer for the sunny slope and shady slope. The above plots (a–g) are from the LRCC analysis method, which use a polynomial order of 1 to fit the global trend. The $\log_2 (F_{cor}(w))$ is as a function of $\log_2 w$ (w corresponding to the timescale). The point of the cross correlation in shady slope is represented by the blue triangle, and the point of cross correlation in sunny slope is represented by the red circle. The value of H_{cor} is the slope of the line. There are two slopes for each depth, and the inflection point is the last point on the first interval (i.e., the green circle in figure (a)). Inflection point exists at $\log_2 w = 2.7004$ at each depth. H_{cor} fitted by dashed line covers a small timescale ($2 < d < 6$). For depths 4–40 cm, H_{cor} fitted by solid line covers a timescale range 6–65 day. And the points after the black vertical dotted line belong to the third region. For depths 80–160 cm, H_{cor} fitted by solid line covers a timescale range over 6 days.

temperature series and moisture series. There is an obvious linear relationship between $F_{cor}(w)$ and w under the double logarithmic coordinates. At a specific depth and specific timescale, LRCC indices of the two slopes are different. Therefore, the cross correlation between these two series has a multiple timescale property. This indicates that there is consistent change between these two series. In addition, there is an inflection point in fitting H_{cor} at each depth and H_{cor} varies with depth. This means that the LRCC between the soil temperature and moisture displays the timescale variation and vertical depth variation.

From Figure 6, for the sunny slope and shady slope, the intensity of the consistency both mutates at 6 days on the timescale. There is the same timescale variation of the LRCC at the two slopes. It can be fitted out of two H_{cor} indices (slopes). The fast scaling region covers time windows from 1.3219 to 2.7004 (2- to 6-day estimates). There is consistency between these two series only at 4- to 20-cm depths at the two slopes and 160-cm depth at the sunny slope. For 4- to 40-cm depths, the slow scaling region covers time windows of 2.7004–6.0334 (6- to 65-day estimates). The third region (time windows over 6.0334) is not fitted. For depth 80–160 cm, the slow scaling region covers the range over 6 days. There is a consistency at most depths.

Consistency between these two series is mainly displayed in a slow scaling region (6–65 days). To analyze the vertical depth variation of the LRCC at the two slopes, H_{cor} of the slow scaling region at the two slopes was plotted in Figure 7.

From Figure 7, on both the sunny slope and shady slope, the LRCC indices demonstrate a vertical depth variation. Meanwhile, the intensity of consistency increases with depth and this phenomenon is more obvious in the shady slope. For the sunny slope, there is antipersistence in 4-cm depth. The consistency strengthens with depth from 10 to 40 cm. There is no LRCC at 80-cm depth. The strongest consistency is at 120-cm depth ($H_{cor} = 0.953$). For the shady slope, the consistency basically strengthens with depth. The consistency reaches a maximum at 120-cm depth ($H_{cor} = 0.909$). For the 4- to 40-cm depths, the

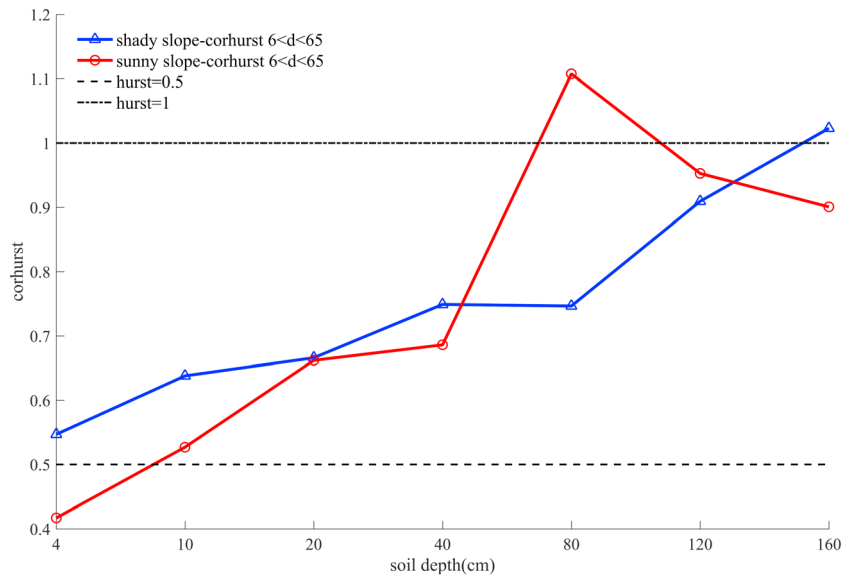


Figure 7. Comparison of soil moisture-temperature H_{cor} between the sunny slope and shady slope. The longitudinal axis represents the value of the H_{cor} , and the horizontal axis represents different depths. The red and blue lines correspond to the H_{cor} results of different sunshine conditions, sunny slope, and shady slope, respectively.

consistency on the shady slope is stronger than that on the sunny slope, and the 120-cm depths are in contrast.

5. Discussion and Conclusions

5.1. Discussion

The reasons of the timescale variation and the vertical depth variation of LRC and LRCC are discussed in this section.

There is the same response rate of soil temperature, soil moisture, and hydrothermal interaction to the influence of external meteorological factors (SR, evapotranspiration [EV], and so on) on the shady slope and sunny slope. The timescale variation of LRC illustrates the response rate of the soil moisture or temperature to external meteorological factors. The timescale variation of LRCC results illustrates the response rate of the hydrothermal interaction to SR. The inflection points of H or H_{cor} for the two slopes appear on the same timescale. No matter it is soil moisture or soil temperature, the intensity of its persistence changes at the same timescale for the two slopes. And the consistency intensity between them also changes at the same timescale for the two slopes.

The vertical depth variation of the LRC and LRCC in shallow layer is mainly affected by hydrothermal interaction driven by SR. The SR condition is significantly different between the shady and sunny slope. By comparing the LRC and LRCC results between the two slopes in the slow scaling region, both LRC indices and LRCC indices are different on the two slopes. SR impacts the soil moisture and temperature series by affecting the hydrothermal interaction, especially in the shallow layer (Atchley & Maxwell, 2011; Helm et al., 2016). There are two main aspects of the hydrothermal interaction in the soil: On the one hand, with the increase of SR, soil temperature increases. And then, the EV of soil and vegetation increases and soil moisture is reduced (Atchley et al., 2011; Zhang et al., 2001). The quantity of surface EV is mainly influenced by the soil temperature and the soil moisture of the shallow soil. Soil moisture affects water supply of vegetation (Huber et al., 2014). Most of the water absorbed from the soil by vegetation roots is used for transpiration. If the soil moisture is too low, plants cannot conduct normal transpiration (Barigah et al., 2013). The research of Laio et al. (2001) has given the detailed introduction how EV is reduced with decreasing soil moisture within the rooting zoon. Soil temperature also has a significant effect on the transpiration rate of vegetation (Wang et al., 2015), but the increase or decrease of the transpiration rate with the soil temperature depends on the range of soil temperature. Soil surface evaporation is directly affected by soil moisture.

Soil temperature affects the soil surface evaporation by affecting latent heat and sensible heat flux. On the other hand, the soil EV process can adjust the energy balance of soil system (Li et al., 2015; Villegas et al., 2009). The EV process can weaken the increase of soil temperature to a certain extent (Atchley & Maxwell, 2011; Fan et al., 2003).

For the shallow layer, the soil moisture LRC and the soil temperature LRC are mainly affected by the SR and evaporation. For the soil moisture, the shallow water content is mainly used for soil surface evaporation and plant transpiration, and thus, it is sensitive to SR changes (Stearns & Carlson, 1960). The sunny slope received more SR than the shady slope. Therefore, the soil moisture of the sunny slope is more affected by the SR, and the persistence of soil moisture on the sunny slope was significantly lower than that on the shady slope in shallow layer. For the soil temperature, it is directly affected by the SR and (Gao et al., 2005). In addition, soil temperature is indirectly affected by soil EV. The EV in soil surface has a negative feedback regulation on the soil temperature (Fan et al., 2003; Atchley & Maxwell, 2011). The more active the EV process is, the stronger this negative feedback regulation is to the soil temperature. Therefore, the soil temperature series displays antipersistence at the slow timescale in 4- to 20-cm depth, 4-cm depth with the strongest antipersistence. Because of the stronger SR at the sunny slope, the antipersistence of soil temperature on the sunny slope is stronger than that on the shady slope. Interaction between soil temperature and moisture is also affected by the SR and EV (Lakshmi et al., 2010). The soil temperature increases with the SR. It results in a phase transformation of soil water, and the soil temperature is reduced in turn (Al Kayssi et al., 1990; Atchley & Maxwell, 2011). The high intensity of this hydrothermal interaction is represented as a low consistency. In the shallow layer, because of the stronger SR on the sunny slope, there is the more significant hydrothermal interaction on the sunny slope. Therefore, for the shallow layer on the sunny slope, the tendency of soil moisture to rise with temperature is inhibited more significantly and there is lower consistency. Especially for 4-cm depth in sunny slope, there is anticonsistency because of the strongest hydrothermal interaction. The influence of the SR on the soil elements weakens with the depth (Fan et al., 2003). Therefore, for both the soil moisture and the soil temperature, the persistence or antipersistence intensity tends to weaken with the depth. And the consistency between them strengthens with the depth. It illustrates that intensity of interaction between them also descends with the depth. In addition, Cheng et al. (2009) proved that roots of cold season grass were distributed above the 20-cm depth. That means the influence range of plant transpiration is mainly in the shallow layer. It is also indicated that the influence range of SR on soil elements is mainly concentrated in shallow layer.

For the middle layer, soil moisture persistence can be affected by a variety of factors including groundwater recharge (GDR) and side runoff supply. The GDR and side runoff have influence on soil moisture by affecting the water supply (Guo et al., 2010; Zhu et al., 2015). The sunny slope station is closer to the runoff. While, less runoff is distributed around the shady slope station. Water supply for sunny slope is more stable than that for shady slope. Therefore, the persistence of the soil moisture in the shady slope is obviously weaker than that on the sunny slope in this layer. The moisture series on the shady slope shows the higher level of noise. In addition, although there is the same vegetation type on shady and sunny slopes, sunny slopes have better growth conditions (sufficient SR and stable water supply), which may make the number and coverage of vegetation on sunny slopes higher than on shady slopes. As a result, the infiltration rate of precipitation and surface runoff is faster in shady slope. This also weakens the persistence in 80-cm shady slope and improves its noise level. Hydrothermal interaction intensity in sunny is slightly affected by SR in this layer. The effect of SR on soil elements tends to disappear over 40-cm depth, weakening with the depth (Fan et al., 2003). There is the more significant hydrothermal interaction on the sunny slope due to the stronger SR. Therefore, the consistency between soil moisture and soil temperature in the sunny slope is also weaker than that on the sunny at 40-cm depth.

For the deep layer, seasonal ice meltwater driven by SR mainly affects the hydrothermal interaction intensity, the soil moisture LRC in the sunny slope. Seasonal meltwater on the sunny slope is less stable within a year because of the amount of SR change. Seasonal ice and snow meltwater directly affect the moisture by affecting the supply of deep soil water (Zhu et al., 2015). Therefore, the persistence of soil moisture on the sunny slope is generally weaker than that on the shady slope. The intensity of the persistence on the sunny slope decreases with the depth in deep layer. Furthermore, the persistence of soil moisture at 160-cm depth is significantly affected. The seasonal meltwater indirectly affects the hydrothermal interaction by affecting the soil moisture. Due to the stronger effect on the sunny slope, the consistency between the soil moisture

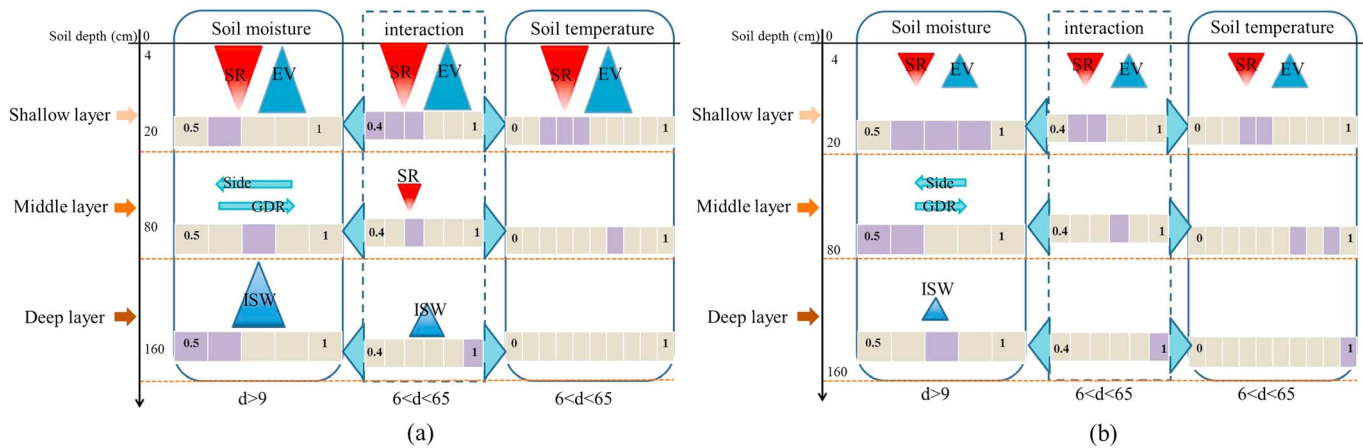


Figure 8. Three-layer structure of soil heat and water long-range correlations and long-range cross correlation. The arrows of different colors correspond to different factors that affect the soil system in the slow scaling region. The large arrow expresses a strong influence and small arrow expresses a weak influence. A table filled with color represents the value range of H or H_{cor} in a layer. The red arrow represents solar radiation (SR). The light blue arrow represents evapotranspiration (EV). The blue arrow represents the ice and snow meltwater supply (ISW). Green arrows pointing inside and outside represent the side runoff supply (Side) and groundwater recharge (GDR), respectively.

and the soil temperature on the sunny slope weakens with depth in deep layer. The intensity of consistency on the sunny slope is considerably lower than that on the shady slope at 160-cm depth.

According to the above results, the vertical depth variation in different layers is illustrated in Figure 8. At large timescales, each layer has its own main influence factors, and these factors can be used to explain the difference in H or H_{cor} between the two slopes. In the shallow layer, the soil moisture, soil temperature, and the interaction between them are all affected by SR and EV. In addition, these indicators have a stronger effect on the sunny slope. In the middle layer, soil water is supplied by side runoff (Side) and GDR. These factors have a stronger effect on the soil moisture on the sunny slope. In the deep layer, ice and snow meltwater supply main influence factor in this layer. Moreover, it has the strongest influence on the soil moisture for the sunny slope, then on the soil temperature and hydrothermal interaction for the sunny slope, and the weakest influence on the moisture is for the shady slope.

5.2. Conclusions

In this study, the soil was stratified to calculate the indices of LRCC and LRC at different depths. The H indices of soil moisture and soil temperature and H_{cor} between them were compared between different sunshine conditions. LRCC between the soil temperature and moisture and LRC of the soil temperature or moisture illuminated the vertical depth variation and timescale variation.

Based on the LRC and LRCC results, there are three common characteristics in the sunny slope and the shady slope.

First, the fluctuation of soil temperature or moisture is not completely random. At the slow timescale, the soil moisture series displays persistence in all depths. The soil temperature series displays antipersistence in shallow layer and persistence in the other layers. Soil temperature and moisture are not independent but with consistent change in nearly all depths.

Second, for all depths on the two slopes, the persistence or antipersistence intensity of soil temperature changes over 6 days, the persistence intensity of soil moisture changes over 9 days, and the consistency intensity between soil temperature and soil moisture changes over 6 days. The response rate of soil temperature or soil moisture or interaction between them to external factors is the same on the two slopes.

Third, LRC and LRCC indices all show stratification heterogeneity. For the two slopes, the persistence of soil moisture strengthens with depth in shallow layer; the antipersistence of soil temperature decreases with depth in shallow layer and the persistence increases with depth in the other layers; the consistency between them strengthens with depth in shallow layer.

While, LRC and LRCC results on the two slopes also have differences. The soil system can be stratified to three layers to explain these differences over the large timescales, which is described in Figure 8. Three conclusions are summarized.

First, for soil moisture, the persistence of the shady slope is stronger than that of the sunny slope in the shallow layer because of less solar radiation and evapotranspiration affects. In the middle layer, groundwater recharge and side runoff supply are more stable on the sunny slope, and thus, it results in the stronger persistence of soil moisture on the sunny slope. In the deep layer, because the seasonal meltwater driven by solar radiation has a stronger influence on the sunny slope, the persistence of soil moisture on the sunny slope was considerably weaker than that on the shady slope. In addition, the persistence on the sunny slope weakens with depth, whereas the persistence on the shady slope is the opposite.

Second, for soil temperature, in the shallow layer, because of the stronger hydrothermal interaction driven by solar radiation and evapotranspiration on the sunny slope, antipersistence of soil temperature on the sunny slope is stronger than that on the shady slope. In the middle layer, the persistence of soil temperature on the sunny slope is similar with that on the shady slope. In the deep layer, the persistence of soil temperature on the shady slope slightly strengthens with depth.

Third, for interactions between soil temperature and moisture, in the shallow layer, because of stronger solar radiation on the sunny slope, the consistency between the two series on the sunny slope is weaker than that on the shady slope. In the middle layer, the consistency on the shady slope is stronger than that sunny on the slope at 40-cm depth, with the effect of solar radiation on the sunny slope. In the deep layer, with indirect meltwater influence on the sunny slope, the consistency on the sunny slope slightly weakens with depth, whereas consistency on the shady slope is the opposite.

In addition, there are many other contents worth further study. For example, the relationship between the future trend and the past trend of soil temperature at 80- to 160-cm depths sunny slope cannot be explained by the LRC analysis. This may be more related to the soil structure, thermodynamic properties, and so on. For 80-cm depth on the sunny slope, there is no interaction between soil moisture and soil temperature. The reason behind this may be related to the change of the soil hydrothermal process in this depth and still needs further investigation.

LRC indices can reflect the predictability of series (Zhu et al., 2010). By quantifying the intensity of persistence, the predictability of soil temperature and moisture can be reflected under different timescales to a certain extent. Adding the timescale characteristics of variables to the climate model can improve the simulation results of the model (Blender & Fraedrich, 2003; Bunde et al., 2001). There is higher predictability for the series with higher persistence intensity. Through the above results, it can be found that LRC of soil moisture, LRC of soil temperature, and LRCC between soil moisture and temperature all display vertical depth and timescale variations. The intensity of persistence or antipersistence may change at different timescales and different depths. This phenomenon may exist in other regions. When used in potential modeling, managing, or monitoring approach, researchers can preselect time windows and soil depths with higher LRC indices. It is more reliable for the simulation and prediction of indicators related to soil based on soil depth and the natural environment with stronger persistence.

In addition, this study takes the typical geographical environment as an example and reveals the potential influence of external meteorological factors on predictability of soil moisture and soil temperature. Such potential influence also exists in other regions, but the intensity and significance of the influence are different. Through the comparison of LRC and LRCC results from these two different geographical environments, this study analyzed the influence process of meteorological factors (solar radiation, evapotranspiration, and so on) on stratification heterogeneity of LRC and LRCC. The parameters related to the soil in land surface process models are set in advance according to empirical values or model calibration presently. While, in the determination of soil water and heat optimum parameters, the potential influence of meteorological factors should also be considered. The above conclusions can assist parameter optimization in modeling under different meteorological conditions (sunshine, evaporation, etc.).

In this study, the influence of external meteorological factors on soil system is qualitatively analyzed. In fact, meteorological factors play an important role in soil system research, and they will affect the evolutionary trend characteristics of soil moisture and temperature series. Combination of meteorological data, the influence of them on the soil system could be considered quantitatively in the future.

Acknowledgments

This work was supported by the National Key R&D Program of China (2017YFA0604704), National Natural Science Foundation of China (91725000), and the Fundamental Research Funds for the Central Universities. The data used in this study are available from Environmental and Ecological Science Data Center for West China at <http://www.heihedata.org/>.

References

Al Kayssi, A. W., Al Karaghoul, A. A., Hasson, A. M., & Beker, S. A. (1990). Influence of soil moisture content on soil temperature and heat storage under greenhouse conditions. *Journal of Agricultural Engineering Research*, 45(4), 241–252. [https://doi.org/10.1016/S0021-8634\(05\)80152-0](https://doi.org/10.1016/S0021-8634(05)80152-0)

Albergel, C., Dorigo, W., Reichle, R. H., Balsamo, G., de Rosnay, P., Muñoz-Sabater, J., et al. (2013). Skill and global trend analysis of soil moisture from reanalyses and microwave remote sensing. *Journal of Hydrometeorology*, 14(4), 1259–1277. <https://doi.org/10.1175/JHM-D-12-0161.1>

Atchley, A. L., & Maxwell, R. M. (2011). Influences of subsurface heterogeneity and vegetation cover on soil moisture, surface temperature and evapotranspiration at hillslope scales. *Hydrogeology Journal*, 19(2), 289–305. <https://doi.org/10.1007/s10040-010-0690-1>

Barigah, T. S., Charrier, O., Douris, M., Bonhomme, M., Herbette, S., Améglio, T., et al. (2013). Water stress-induced xylem hydraulic failure is a causal factor of tree mortality in beech and poplar. *Annals of Botany*, 112(7), 1431–1437. <https://doi.org/10.1093/aob/mct204>

Biswas, A., Zeleke, T. B., & Si, B. C. (2012). Multifractal detrended fluctuation analysis in examining scaling properties of the spatial patterns of soil water storage. *Nonlinear Processes in Geophysics*, 19(1), 1–12.

Blender, R., & Fraedrich, K. (2003). Long time memory in global warming simulations. *Geophysical Research Letters*, 30(14), 1769. <https://doi.org/10.1029/2003GL017666>

Bunde, A., Havlin, S., Koscielny-Bunde, E., & Schellnhuber, H. J. (2001). Long term persistence in the atmosphere: Global laws and tests of climate models. *Physica A: Statistical Mechanics and its Applications*, 302(1–4), 255–267. [https://doi.org/10.1016/S0378-4371\(01\)00469-1](https://doi.org/10.1016/S0378-4371(01)00469-1)

Chahine, M. T. (1992). The hydrological cycle and its influence on climate. *Nature*, 359(6394), 373–380. <https://doi.org/10.1038/359373a0>

Changqing, S., Changxiu, C., & Peijun, S. (2018). Geography complexity: New connotations of geography in the new era [J]. *Acta Geographica Sinica*, 73(7), 1204–1213.

Changxiu, C., Peijun, S., Changqing, S., & Jianbo, G. (2018). Geographic big-data: A new opportunity for geography complexity study [J]. *Acta Geographica Sinica*, 73(8), 1397–1406.

Che, Z., Jinjun, L. I., Wang, Y., Ding, G., Shixia, L. I., Hua, D. I., et al. (2018). Characteristics of soil temperature and water content variation in the western qilian mountains. *Ecologica Sinica*, 38(1).

Cheng, W. J., Cui, J. Y., Min, F. H., & Hu, L. (2009). Root distribution characteristics of three turfgrasses and their impact on soil nutrient content. *Acta Prataculturae Sinica*, 18(01), 179–183.

Dai, A. (2013). Increasing drought under global warming in observations and models. *Nature Climate Change*, 3(1), 52–58. <https://doi.org/10.1038/nclimate1633>

Ding, J., Zhao, W., Daryanto, S., Wang, L., Fan, H., & Feng, Q. (2017). The spatial distribution and temporal variation of desert riparian forests and their influencing factors in the downstream heihe river basin, china. *Hydrology & Earth System Sciences*, 21(5) 1–27.

Fan, A., Wei, L., & Wang, C. (2003). Simulation on the daily change of soil temperature under various environment conditions. *Acta Energiæ Solaris Sinica*, 24(2), 167–171.

Gao, J., Fang, P., & Liu, F. (2017). Empirical scaling law connecting persistence and severity of global terrorism. *Physica A: Statistical Mechanics and its Applications*, 482, 74–86. <https://doi.org/10.1016/j.physa.2017.04.032>

Gao, J., Hu, J., & Tung, W. (2011). Facilitating joint chaos and fractal analysis of biosignals through nonlinear adaptive filtering. *PLoS One*, 6(9), 1–8.

Gao, J., Jing, H., Xiang, M., & Perc, M. (2012). Culturomics meets random fractal theory: Insights into long-range correlations of social and natural phenomena over the past two centuries. *Journal of the Royal Society Interface*, 9(73), 1956–1964. <https://doi.org/10.1098/rsif.2011.0846>

Gao, J., Lasch, E. B., & Chen, Q. (2013). Multiscale analysis to facilitate joint chaos and fractal analysis of biosignals. *IEEE Aerospace and Electronics Conference*, 8347, 96–102.

Gao, J., Leetaru, K. H., Hu, J., Cioffi-Revilla, C., & Schrodt, P. (2013). Massive media event data analysis to assess world-wide political conflict and instability. In *Social computing, behavioral-cultural modeling and prediction* (pp. 284–292). Berlin: Springer. https://doi.org/10.1007/978-3-642-37210-0_31

Gao, X. F., Liu, Y. H., Guo, J. Q., Hao, L. Y., & Wang, Y. Y. (2015). Research on change of soil moisture content based on detrended fluctuation analysis. *The Soil*, 47(01), 188–191.

Gao, Z., Bian, L., & Liu, S. (2005). Flux measurements in the near surface layer over a non-uniform crop surface in China. *Hydrology and Earth System Sciences Discussions*, 2(3), 1067–1085. <https://doi.org/10.5194/hessd-2-1067-2005>

Goodchild, M. F., & Mark, D. M. (2015). The fractal nature of geographic phenomena. *Annals of the Association of American Geographers*, 77(2), 265–278.

Green, F. H. W., Harding, R. J., & Oliver, H. R. (2010). The relationship of soil temperature to vegetation height. *International Journal of Climatology*, 4(3), 229–240.

Guo, F. F., Nan, L., Chen, A. Q., & Liu, G. C. (2010). Influence of vegetation coverage on surface runoff and soil moisture in rainy season in dry-hot valley. *Journal of Anhui Agricultural Sciences*, 11(4), 138–143.

Han, L., Chen, H., Chen, T., Yangyang, F. U., & Yang, L. I. (2016). Variations of the soil temperature and moisture in qaidam basin and their relationship. *Research of Soil & Water Conservation*, 23(6), 166–173.

He, H. D., Wang, J. L., Wei, H. R., Ye, C., & Ding, Y. (2016). Fractal behavior of traffic volume on urban expressway through adaptive fractal analysis. *Physica A: Statistical Mechanics and its Applications*, 443, 518–525. <https://doi.org/10.1016/j.physa.2015.10.004>

Helm, P., Stirling, R., & Glendinning, S. (2016). The implications of using estimated solar radiation on the derivation of potential evapotranspiration and soil moisture deficit within an embankment. *Procedia Engineering*, 143, 697–707. <https://doi.org/10.1016/j.proeng.2016.06.105>

Huber, K., Vanderborght, J., Javaux, M., Schröder, N., Dodd, I. C., & Vereecken, H. (2014). Modelling the impact of heterogeneous rootzone water distribution on the regulation of transpiration by hormone transport and/or hydraulic pressures. *Plant and Soil*, 384(1–2), 93–112. <https://doi.org/10.1007/s11104-014-2188-4>

Joelson, M., Golder, J., Beltrame, P., Néel, M. C., & di Pietro, L. (2016). On fractal nature of groundwater level fluctuations due to rainfall process. *Chaos, Solitons & Fractals*, 82, 103–115. <https://doi.org/10.1016/j.chaos.2015.11.010>

Katul, G. G., Oren, R., Manzoni, S., Higgins, C., & Parlange, M. B. (2012). Evapotranspiration: A process driving mass transport and energy exchange in the soil-plant-atmosphere-climate system. *Reviews of Geophysics*, 50, RG3002. <https://doi.org/10.1029/2011RG000366>

Kim, S., & Singh, V. P. (2014). Modeling daily soil temperature using data-driven models and spatial distribution. *Theoretical and Applied Climatology*, 118(3), 465–479. <https://doi.org/10.1007/s00704-013-1065-z>

Koster, R. D., Dirmeyer, P. A., Guo, Z., Bonan, G., Chan, E., Cox, P., Gordon, C. T., et al., & GLACE Team (2004). Regions of strong coupling between soil moisture and precipitation. *Science*, 305(5687), 1138–1140. <https://doi.org/10.1126/science.1100217>

- Laio, F., Porporato, A., Ridolfi, L., & Rodriguez-Iturbe, I. (2001). Plants in water-controlled ecosystems: Active role in hydrologic processes and response to water stress- II. Probabilistic soil moisture dynamics. *Advances in Water Resources*, *24*(7), 707–723. [https://doi.org/10.1016/S0309-1708\(01\)00005-7](https://doi.org/10.1016/S0309-1708(01)00005-7)
- Lakshmi, V., Jackson, T. J., & Zehrhuhs, D. (2010). Soil moisture–temperature relationships: Results from two field experiments. *Hydrological Processes*, *17*(15), 3041–3057.
- Li, G. W., Feng, Q., Zhang, F. P., & Cheng, A. F. (2014). The soil infiltration characteristics of typical grass land in babao river basin of qilian mountain. *Agricultural Research in the Arid Areas*, *32*(1), 60–65.
- Li, X., Cheng, G. D., Liu, S. M., Xiao, Q., Ma, M., Jin, R., et al. (2013). Heihe Watershed Allied Telemetry Experimental Research (HiWATER): Scientific objectives and experimental design. *Bulletin of the American Meteorological Society*, *94*(8), 1145–1160. <https://doi.org/10.1175/BAMS-D-12-00154.1>
- Li, Y., Zhou, J., Wang, H., Li, D., Jin, R., Zhou, Y., & Zhou, Q. (2015). Integrating soil moisture retrieved from L-band microwave radiation into an energy balance model to improve evapotranspiration estimation on the irrigated oases of arid regions in northwest China. *Agricultural and Forest Meteorology*, *214–215*, 306–318.
- Liu, S. M., Xu, Z. W., Wang, W. Z., Jia, Z. Z., Zhu, M. J., Bai, J., & Wang, J. M. (2011). A comparison of eddy-covariance and large aperture scintillometer measurements with respect to the energy balance closure problem. *Hydrology and Earth System Sciences*, *15*(4), 1291–1306. <https://doi.org/10.5194/hess-15-1291-2011>
- Mandelbrot, B. B. (1991). *The fractal geometry of nature*. Birkhauser Verlag.
- Mandelbrot, B. B., & Wallis, J. R. (1995). Some-long-run properties of geophysical records. In *Fractals in the Earth Sciences* (pp. 321–340). Boston, MA: Springer.
- Peng, C. K., Buldyrev, S. V., Havlin, S., Simons, M., Stanley, H. E., & Goldberger, A. L. (1994). Mosaic organization of DNA nucleotides. *Physical Review E*, *49*(2), 1685–1689. <https://doi.org/10.1103/PhysRevE.49.1685>
- Podobnik, B., Jiang, Z. Q., Zhou, W. X., & Stanley, H. E. (2011). Statistical tests for power-law cross-correlated processes. *Physical Review E, Statistical, Nonlinear, and Soft Matter Physics*, *84*(2), 066–118.
- Podobnik, B., & Stanley, H. E. (2008). Detrended cross-correlation analysis: A new method for analyzing two non-stationary time series. *Physical Review Letters*, *100*(8), 084–102.
- Porporato, A., D'Odorico, P., Laio, F., Ridolfi, L., & Rodriguez-Iturbe, I. (2002). Ecohydrology of water-controlled ecosystems. *Advances in Water Resources*, *25*(8–12), 1335–1348. [https://doi.org/10.1016/S0309-1708\(02\)00058-1](https://doi.org/10.1016/S0309-1708(02)00058-1)
- Riley, M. A., Bonnette, S., Kuznetsov, N., Wallot, S., & Gao, J. (2012). A tutorial introduction to adaptive fractal analysis. *Frontiers in Physiology*, *3*, 371.
- Seneviratne, S. I., Corti, T., Davin, E. L., Hirschi, M., Jaeger, E. B., Lehner, I., et al. (2010). Investigating soil moisture-climate interactions in a changing climate: A review. *Earth-Science Reviews*, *99*(3–4), 125–161. <https://doi.org/10.1016/j.earscirev.2010.02.004>
- Sheffield, J., & Wood, E. F. (2010). Global trends and variability in soil moisture and drought characteristics, 1950–2000, from observation-driven simulations of the terrestrial hydrologic cycle. *Journal of Climate*, *21*(3), 432–458.
- Shen, S., Ye, S., Cheng, C., Song, C., Gao, J., Yang, J., et al. (2018). Persistence and 669 corresponding time scales of soil moisture dynamics during summer in the Babao River 670 Basin, Northwest China. *Journal of Geophysical Research: Atmospheres*, *123*, 1–13. <https://doi.org/10.1029/2018JD029094>
- Song, C. Q., Yuan, L. H., Yang, X. F., & Bojie, F. U. (2017). Ecological-hydrological processes in arid environment: Past, present and future. *Journal of Geographical Sciences*, *27*(12), 1577–1594. <https://doi.org/10.1007/s11442-017-1453-x>
- Song, R. L., Yu, J. J., & Liu, C. M. (2011). Long-range correlations of soil moisture series with detrended fluctuation analysis. *Journal of Hydraulic Engineering*, *42*(3), 315–322.
- Song, X., Leng, P., Li, X., Li, X., & Ma, J. (2013). Retrieval of daily evolution of soil moisture from satellite-derived land surface temperature and net surface shortwave radiation. *International Journal of Remote Sensing*, *34*(9–10), 3289–3298. <https://doi.org/10.1080/01431161.2012.716915>
- Sorman, A. U., & Abdulrazzak, M. J. (2010). Estimation of actual evaporation using precipitation and soil moisture records in arid climates. *Hydrological Processes*, *9*(7), 729–741.
- Stearns, F. W., & Carlson, C. A. (1960). Correlations between soil-moisture depletion, solar radiation, and other environmental factors. *Journal of Geophysical Research*, *65*(11), 3727–3732. <https://doi.org/10.1029/JZ065i011p03727>
- Tang, Z. X., He, Z. B., & Liu, H. (2012). Soil moisture and temperature characteristics of forest-grassland ecotone in middle Qilian Mountains and the responses to meteorological factors. *Acta Ecologica Sinica*, *32*(4), 1056–1065. <https://doi.org/10.5846/stxb201010091418>
- Trenberth, K. E., Dai, A., Schrier, G. V. D., Jones, P. D., Barichivich, J., Briffa, K. R., & Sheffield, J. (2014). Global warming and changes in drought. *Nature Climate Change*, *4*(1), 17–22.
- Villegas, J. C., Breshears, D. D., Zou, C. B., & Law, D. J. (2009). Ecohydrological controls of soil evaporation in deciduous drylands: How the hierarchical effects of litter, patch and vegetation mosaic cover interact with phenology and season. *Journal of Arid Environments*, *74*(5), 595–602.
- Wang, G., Dolman, A. J., Blender, R., & Fraedrich, K. (2010). Fluctuation regimes of soil moisture in ERA-40 re-analysis data. *Theoretical and Applied Climatology*, *99*(1–2), 1–8. <https://doi.org/10.1007/s00704-009-0111-3>
- Wang, J., Zhu, Z., Song, X., & Hongjin, Z. (2015). The effects of the soil temperature and moisture on the evapotranspiration of yellow willows in Hunshandak sand area. *Journal of Arid Land Resources & Environment*, *29*(01), 77–82.
- Williams, D. G. (2013). Ecohydrology of water-controlled ecosystems : Soil moisture and plant dynamics. *Eos Transactions American Geophysical Union*, *86*(38), 344–344.
- Wu, X., Yao, Z., Brüggemann, N., Shen, Z. Y., Wolf, B., Dannenmann, M., Zheng, X., et al. (2010). Effects of soil moisture and temperature on CO₂ and CH₄ soil-atmosphere exchange of various land use/cover types in a semi-arid grassland in Inner Mongolia, China. *Soil Biology & Biochemistry*, *42*(5), 773–787. <https://doi.org/10.1016/j.soilbio.2010.01.013>
- Yang, L., Chen, L., & Wei, W. (2015). Effects of vegetation restoration on the spatial distribution of soil moisture at the hillslope scale in semi-arid regions. *Catena*, *124*(1), 138–146. <https://doi.org/10.1016/j.catena.2014.09.014>
- Zhang, L., Dawes, W. R., & Walker, G. R. (2001). Response of mean annual evapotranspiration to vegetation changes at catchment scale. *Water Resources Research*, *37*(3), 701–708. <https://doi.org/10.1029/2000WR900325>
- Zhu, X., Fraedrich, K., Liu, Z., & Blender, R. (2010). A demonstration of long-term memory and climate predictability. *Journal of Climate*, *23*(18), 5021–5029. <https://doi.org/10.1175/2010JCLI3370.1>
- Zhu, Y., Zhao, X., Chen, M., Luo, Y., & Zhou, X. (2015). Effects of different land uses on spatial variability of soil moisture under freeze-thaw action. *Journal of Irrigation & Drainage*, *34*(05), 51–54.



Journal |  Articles

Actions

JGR Atmospheres

Impact factor: 3.38

Online ISSN: 2169-8996

JGR: Atmospheres

Featured Articles

Browse Articles

Recently Published

Accepted Articles

Most Cited

[Free Access](#)

[Issue Information](#)

[Abstract](#) | [Full text](#) | [PDF](#) | [Request permissions](#)

Full Access

The Implications for Radiative Cloud Forcing via the Link Between Shallow Convection and Planetary Boundary Layer Mixing

- , Y. C. Kwon

Journal of Geophysical Research: Atmospheres | First Published:   November  0 

[Abstract](#) | [Full text](#) | [PDF](#) | [References](#) | [Request permissions](#)

Key Points

- PBL mixing and shallow convection are tightly linked in model
 - Intensity of diffusivity profile in shallow convection scheme can modulate cloud amount and radiation budget
 - NWP performance can conventionally be improved via a modification of shallow convection scheme
-

Full Access

Interannual Variation and Regime Shift of the Evaporative Moisture Sources for Wintertime Precipitation Over Southern China

Zifan Yang, Wenyu Huang , Tianpei Qiu, Xinsheng He, Jonathon S. Wright, Bin Wang

Journal of Geophysical Research: Atmospheres | First Published:   November  0 

[Abstract](#) | [Full text](#) | [PDF](#) | [References](#) | [Request permissions](#)

Key Points

- The moisture contribution from the South China Sea is modulated by the circulation pattern rather than evaporation from ocean surface
 - The two types of El Nino have distinct impacts on the moisture contribution
 - An eastward migration of the moisture source occurred during 1991/1992, owing to the Maritime Continent warming
-

Free Access

Issue Information

Journal of Geophysical Research: Atmospheres | Pages:          |

First Published:   November  0 

[Abstract](#) | [Full text](#) | [PDF](#) | [Request permissions](#)

[Full Access](#)

Effects of Shape and Rotation of Sand Particles in Saltation

Hongchao Dun, Ning Huang, Jie Zhang, Wei He

Journal of Geophysical Research: Atmospheres | First Published: November 0, 2018

[Abstract](#) | [Full text](#) | [PDF](#) | [References](#) | [Request permissions](#)

Key Points

-
-
-

[Full Access](#)

--

Vineel Yettella, Mark R. England

Journal of Geophysical Research: Atmospheres | First Published: November 0, 2018

[Abstract](#) | [Full text](#) | [PDF](#) | [References](#) | [Request permissions](#)

Key Points

- Internal variability renders the detection of future changes in the seasonal cycle of surface temperature difficult over many regions
- Europe, North Africa, and Siberia, however, exhibit remarkably robust and easily detectable changes across climate model ensembles
- The robust changes over the three regions are primarily driven by changes in surface longwave and turbulent heat fluxes

[Open Access](#)

Evaluations and Improvements of GLDAS2.0 and GLDAS2.1 Forcing Data's Applicability for Basin Scale Hydrological Simulations in the Tibetan Plateau

Wei Qi, Junguo Liu, Deliang Chen

Journal of Geophysical Research: Atmospheres | First Published: November 0, 2018

[Abstract](#) | [Full text](#) | [PDF](#) | [References](#) | [Request permissions](#)

Key Points

-

-   
- - 

[Full Access](#)

Characteristics of Sundowner Winds Near Santa Barbara, CA, From a Dynamically Downscaled Climatology: Environment and Effects Aloft and Offshore

Craig Smith , Benjamin Hatchett, Michael Kaplan

Journal of Geophysical Research: Atmospheres | First Published:   November  0 

[Abstract](#) | [Full text](#) | [PDF](#) | [References](#) | [Request permissions](#)

Key Points

-
-
- -

[Full Access](#)

Cloudiness and Solar Radiation During the Longest Total Solar Eclipse of the 21st Century at Tianhuangping (Zhejiang), China

Marcos A. Peñaloza-Murillo , Jay M. Pasachoff

Journal of Geophysical Research: Atmospheres | First Published:   November  0 

[Abstract](#) | [Full text](#) | [PDF](#) | [References](#) | [Request permissions](#)

Key Points

- With no solar radiation measurements and cloud direct visual observations an empirical model for global solar radiation has been derived
- This model has been obtained under cloudy skies during the longest total solar eclipse of the 21st century at Tianhuangping (Zhejiang), China
- The results indicate that the solar radiation model is quite acceptable and representative of that which could be have happened at that time

[Full Access](#)

- 

Kai Yang, Chenghai Wang , Shiyue Li

Journal of Geophysical Research: Atmospheres | First Published: November 0

[Abstract](#) | [Full text](#) | [PDF](#) | [References](#) | [Request permissions](#)

Key Points

- Simulation errors are evident in FT process, and CLM4.5 fails to simulate daily and diurnal variation features of soil moisture
- Use of virtual temperature and phase change efficiency effectively improves daily and diurnal variations of soil moisture in FT process
- Consideration of the impact of phase change on soil heat conduction can reduce some soil temperature biases

[MORE >](#)

[Submit an Article](#)

[Get Content Alerts](#)

[Recommend to a Librarian](#)

[Browse Sample Issue](#)

[Subscribe to this Journal](#)

[Special Collections: Call for Papers](#)

Highlights

[A bolt of insight](#)

[Toward More Realistic Modeling of the Mesosphere](#)

[Continental Convection Reaches New Highs](#)

[Spectral Surface Emissivity Improves Arctic Climate Simulation](#)

[See all »](#)

Recent Highlights across AGU Publications

New AGU Publications Site

We want to hear from you! Please share your feedback and help us to continually improve our site.

[Share Feedback](#)

[Call for Papers](#)

[Subsets](#)

[Personal Choice](#)

[Special Section Proposal Form](#)

[Get RSS Feed](#)

[Institutional Subscription Rates](#)

Eos.org: Earth & Space Science News

Earth and Space Science—general Eos feed

- [AGU Announces Locations for the 2019 AGU Fall Meeting and 2020 AGU Fall Meetings](#)
9 Dec 2018
- [Measuring the Magnetic Reconnection Rate in the Magnetotail](#)
8 Dec 2018
- [Introducing the New Editor-in-Chief of GRL](#)
8 Dec 2018
- [Community-Driven Science: Update on the Thriving Earth Exchange](#)
8 Dec 2018
- [AGU Should Support Its Members Who Fly Less](#)
8 Dec 2018



[Read more »](#)

[Download the Multi-journal App](#)



AGU Career Center

AGU PATHFINDER CAREER CENTER

Hydrology Assistantship

Yellowstone National Park, Wyoming | \$400/wk (\$8000 for 20 weeks) + housing + \$250 travel allowance

Employer: National Park Service

Postdoctoral Research Scholar

Boone, North Carolina | Salary is competitive and will be commensurate with qualifications and experience.

Employer: Appalachian State University's Research Institute for Environment, Energy and Economics



Asst/Assoc Professor of Agricultural Hydrology and Water Quality

Wooster, Ohio | Salary commensurate with qualifications

Employer: The Ohio State University



The NASA Postdoctoral Program (NPP)

United States |

Employer: Universities Space Research Association



FDL Intern 2019

Mountain View, California (US) | Stipend

Employer: The SETI Institute



[Back to Top](#)



[AGU PUBLICATIONS](#)

[AGU.ORG](#)

[AGU MEMBERSHIP](#)

[RESOURCES](#)

[PUBLICATION INFO](#)

© 2018 American Geophysical Union

[About Wiley Online Library](#)

[Help & Support](#)

[Opportunities](#)

[Connect with Wiley](#)

Copyright © 1999-2018 John Wiley & Sons, Inc. All rights reserved

WILEY